Brazilian Journal of Technology

Combustion simulation analysis of solid propellant sucrose/potassium nitrate for rocket engine

Análise da simulação de combustão do propelente sólido nitrato de potássio/açúcar para motor foguete

Recebimento dos originais: 17/12/2018
Aceitação para publicação: 29/12/2018

George Stephane Queiroz de Oliveira
Graduando em Engenharia Mecânica pela UFPA
Instituição: Universidade Federal do Parà
Endereço: Rua Augusto Corrêa, 937 - Guamà, Belém – PA, Brasil
georgeoliveira.ufpa@gmail.com

Rene Francisco Boschi Gonçalves
Doutor em Engenharia Aeronâutica e Mecânica pelo ITA
Instituição: Instituto Tecnológico de Aeronáutica, Departamento de Química.
Endereço: Instituto Tecnológico da Aeronáutica, Reitoria, Campus do CTA
12228900 - São José dos Campos, SP - Brasil
renefbg@gmail.com

ABSTRACT

This work presents detail of the process of a solid fuel rocket engine, from the initial hypotheses based on rocket engines with similar characteristics is shown uses simulation software to predict the performance of a solid rocket propellant, where the temperature of combustion products and the products generated by the combustion of propellant based on potassium nitrate and (KNSu) in which it is the product of the reaction of potassium nitrate (KNO_3)/sucrose ($C_{12}H_{22}O_{11}$) were evaluated. The results showed that the values of characteristic exhaust velocity and combustion temperature obtained for the simulation of propellant burning are in agreement with the values found in the literature, The products of the KNSu burning reaction are mostly carbon dioxide, carbon monoxide and water. The simulation used to predict solid rocket propellant performance is a safe and feasible alternative for developing rocket motors.

Keywords: CFD; Rocket engines; Simulation analysis; Spacemodelism.

RESUMO

Este trabalho apresenta detalhe do processo de um motor de foguete de combustível sólido, a partir das hipóteses iniciais baseadas em motores de foguetes com características semelhantes, é utilizado CFD para a simulação para prever o desempenho de um propelente sólido utilizado em foguetes, onde a temperatura de combustão e os produtos gerados com a combustão do propelente a base de nitrato de potássio e açúcar (KNSu) na qual é o produto da reação do potassium nitrate (KNO_3)/sucrose ($C_{12}H_{22}O_{11}$) foram avaliados. Os resultados demonstraram que os valores de velocidade de exaustão característica e temperatura de combustão obtidos para a simulação da queima do propelente estão de

acordo com os valores encontrados na literatura,. Os produtos da reação de queima do KNSu, são em sua maioria dióxido de carbono, monóxido de carbono e água. A simulação utilizada para prever o desempenho do propelente sólido para foguetes é uma alternativa segura e viável para desenvolver motores foguete.

Palavras Chave: CFD; Análise simulacional; motores de foguete; Espaçomodelismo.

1. INTRODUCTION

Unguided rockets are simple construction vehicles. There is no guiding or controlling system and therefore have scatter problems if they are not equipped with suitable correction means. The applications of this type of motors are essentially military-type rockets, air-to-ground and ground-based for military missions, and some civilian applications. In civil applications, they are used, for example, in meteorology or in radioactive components, or to ground the results of telemetry atmospheres. Another of the promising applications is its use as an anti-fire rocket.

The variety of missions that a rocket can carry out is very large and ranges from small applications like attitude control of satellites to engines that drive the first steps of a launch vehicle. The mission of this rocket will be to raise a payload up to a certain height. Rocket motors are autonomous reaction motors, that is, they do not need ambient air for their operation (SHMAKOV *et al.*, 2002). The propulsion is generated by the combustion of an existing mass in the vehicle, called propellant, which leaves the vehicle with a determined amount of associated movement. Therefore, the principle of conservation of the amount of movement, with this action increases the amount of movement of the vehicle in the opposite direction or is counteracted by aerodynamic and gravitational forces. The applications of this type of motors are fundamentally military, rockets air-ground and earth-ground for military missions, and some civil applications. In civil applications they are used, for example, in meteorological or scientific experimentation, such as for the measurement of radioactive components, or in grounding the results of telemetering in atmospheres contaminated by nuclear radiation.

According to the solid rocket motor is designed with the propellant inside the combustion chamber where it is simpler and easier for its handling and storage, however its disadvantage is that these have no control over its combustion after its ignition.

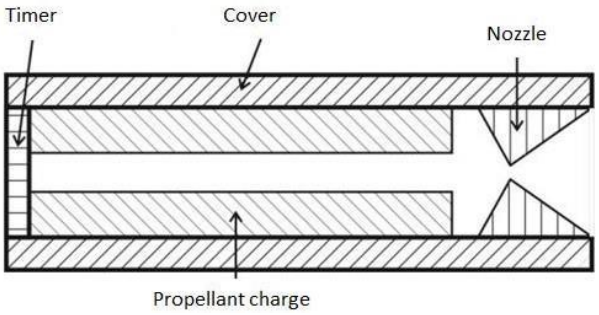

Figure 1 - Scheme of a motor rocket.

The main object of the nozzle is to increase the pressure of the gases resulting from the burning of the propellant, in addition to increasing the escape velocity of the gases, thus raising the thrust of the engine. The timing cover or charge, depending on the case, is intended to prevent the gases from escaping from the side where it is placed if the timing load is chosen, a long firing time must be provided so that an ejector load can be ignited at the end of the load - which can eject the parachute or even the motor.

The potassium nitrate (KNO_3)/sucrose ($C_{12}H_{22}O_{11}$) propellant, is traditionally used in rocket studies by amateur groups. Both components are easy to buy, their combustion products are non-toxic and this propellant can produce relatively high specific impulse, with values higher than the ones obtained by black gunpowder commonly used in model rockets (SHMAKOV *et al.*, 2002).

Traditional methods employed in the production of propellant grains involve fusion (recrystallization) process. In this case, both propellant components are grinded and mixed. After, the mixture is heated until the sucrose fusion around the nitrate grains, forming a doughy mixture which can be placed in molds with a proper propellant grain design, and is cooled in sequence (GUTHEIL , 2011; SUTTON, 2001; PETERSON, 1992; WEISS & SESSLER, 1963; BARRÈRE *et al.* 1960). This methodology produces high density propellant grains (CARTER, 2008), there are, however, risks associated to the propellant combustion by the heating process. Many amateur rocket builders, who use this methodology, consider it secure; nevertheless, it is indispensible the use of equipments that provide a slow and gradual heating process, as well as the control of temperature along the fusion process (LENGELLÉ *et al*., 2000; NAKKA, 1999). The objective of this work was to obtain simulational results of the solid propellant consisting of environmental conditions, thus the absence of a heating process. where the chemical conditions were followed described by Vyvermann (1978). Thus, only the molecular proportion described as the best experimentally obtained was obtained.

2. EXPERIMENTAL PROCEDURE

The computational analysis considered the viscous effects, the reactions of the chemical elements in the combustion process, their path over the motor and the nozzle and the values of the properties at each point within the geometry. Therefore, a mesh was created in reference to the design proposed by Vyvermann (1978), Peterson (1992) and Cornelisse *et al.* (1979).

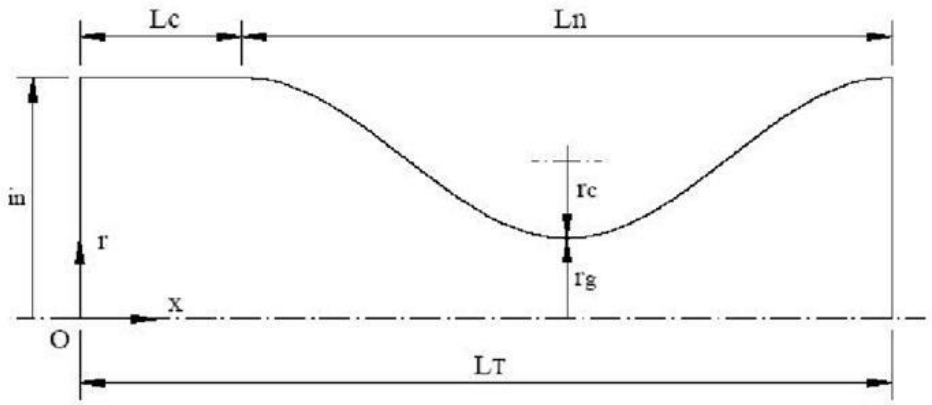

Figure 2 - Geometry of the combustion chambre with the nozzle.

Thus, the geometry of the motor is defined, where:
Rg: Nozzle throat radius (Rg = 0.1m)
Rin: radius of the combustion chamber (Rin = 0.3m)
Rc: radius of curvature (Rc = 4.053x10-2m)
Lc: length of the combustion chamber (Lc = 0,1m)

The initial parameters of the solid propellant rocket motor, prior to the ignition where no changes in the system are possible, are room temperature (25 °C), ambient pressure (1 bar) and a one-dimensional flow.

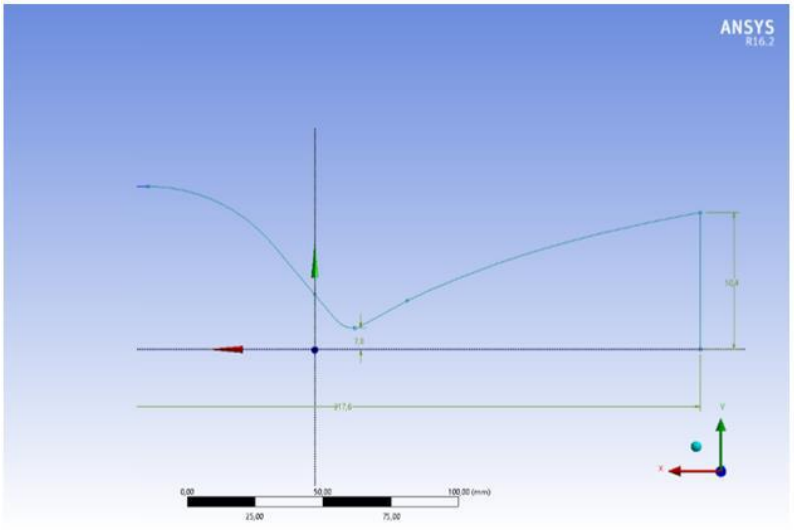

Figure 3 - Technical drawing of the combustion chambre with the nozzle.

A computational analysis of the rocket model to be used was carried out, considering the viscous effects, the reactions of the chemical elements in the combustion process, its routes over the motor and the nozzle, as well as the values of the properties in each point within the geometry.

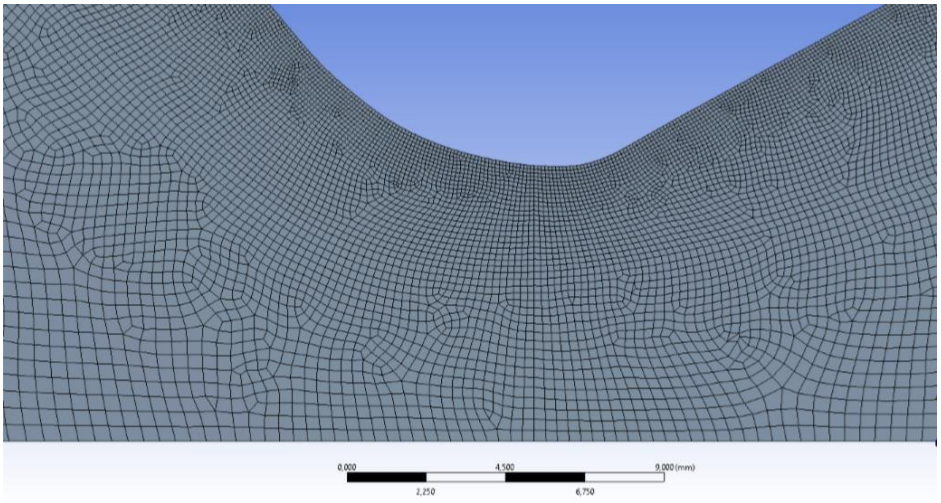

Figure 4 - Mesh refinement in the nozzle throat.

With the initial characteristics inserted, it was necessary to design the mesh for this simulation, in which it was composed by the combustion engine and the propellant material, this was based on an actual motor, that has 110cm of length and the diameter of 25cm, the flow rates of mass at the input and the equivalence ratio is defined as follows in the actual experimental (FOLTRAN *et al.*, 2015). After defining the geometry, the mesh was constructed and it has a mesh according to the parameters found in the literature. The obtained mesh was considered good according to the Ansys commercial code parameters and has 216456 elements and 42376 nodes.

It was necessary to refine the mesh in the area of convergence-divergence in the throat of the nozzle so as to have accuracy when analyzing the physical-chemical and thermal properties, and also to load a certain amount of the reactive chemical elements in the software, to introduce the factors of relaxation to the combustion solution.

With this, the file of the quantities of each chemical element in the combustion reaction was attached, being thus considered. As a propellant, the material of 35% sucrose (sugar, $C_{12}H_{22}O_{11}$) and 65% potassium nitrate (KNO_3), this choice was made on the basis of literature. The form used in the combustion grains was with tubular geometry, because in the experiment Shmakov *et al.* (2002) was realized, for the ease of manufacture and safety of the handling of this propellant, since the matrices for this type of grain are simpler.

Brazilian Journal of Technology

3. COMPUTACIONAL STUDY

The chemical elements were previously mixed, mixing takes place inside the combustion chamber. The process of treatment of energy was non-adiabatic, that is, the particles are free to exchange heat between them. The effects of the compressibility of the fluid were also considered as soon as the combustion started In addition, the diffusion behavior of the flame was treated as being stationary.

The adopted k-ε turbulence models have Eqs. (A) - (B) that allow the determination of the mixing length and time scale by solving two different transport equations, which are present in the k-ε model, in the which has a basis in transport equations for the kinetic energy of turbulence ke and its dissipation rate ε, as shown below:

$$\frac{\partial}{\partial t}(\rho\kappa) + \frac{\partial}{\partial x_i}(\rho\kappa V_i) = \frac{\partial}{\partial x_j}\left[\left(\mu + \frac{\mu_t}{\sigma_\kappa}\right)\frac{\partial\kappa}{\partial x_j}\right] + G_k + G_b - \rho\varepsilon - Y_M + S_k \qquad \text{(A)}$$

$$\frac{\partial}{\partial t}(\rho\varepsilon) + \frac{\partial}{\partial x_i}(\rho\varepsilon V_i) = \frac{\partial}{\partial x_j}\left[\left(\mu + \frac{\mu_t}{\sigma_\varepsilon}\right)\frac{\partial\varepsilon}{\partial x_j}\right] + C_{1\varepsilon}\frac{\varepsilon}{k}(G_k + C_{3\varepsilon}G_b) - C_{2\varepsilon}\rho\frac{\varepsilon^2}{k} + S_k \qquad \text{(B)}$$

In these equations, Gk represents the generation of turbulent kinetic energy due to velocity gradients, Gb the generation of turbulent kinetic energy due to buoyancy, Ym represents the contribution of the floating expansion in compressible turbulent flow to the overall dissipation rate. The feasible K-ε model is also adopted for the work because it presents better performance and therefore can compare the results obtained, as well as the mathematical modeling for transport equations for K and ε is shown in Eq. (C).

$$\frac{\partial k}{\partial t} + U_j\frac{\partial k}{\partial x_j} = \tau_{ij}\frac{\partial U_i}{\partial x_j} - \beta^* k\omega + \frac{\partial}{\partial x_j}\left[(\nu + \sigma^*\nu_T)\frac{\partial k}{\partial x_j}\right] \qquad \text{(C)}$$

With this, the chemical reactions that occur in the combustion process were treated by the combustion model. The chosen model considered the chemical equilibrium, according to the way the

reactants are premixed. In addition, the effect of turbulence has great influence on the flame, making it shorter or longer; these effects are accounted for in the turbulence-chemical interaction.

As the combustion process presents continuous dispersive interactions (gas-liquid and solid-liquid traps), the Discrete Phase Model (MFD) was inserted to consider all the changes resulting from the combustion until its evaporation, since in the process of exchange of heat, the gaseous phase loses energy to the liquid phase, causing the droplet to increase the amount of internal energy to the point where it evaporates.

The gas phase is treated as a continuum, solving equations of mass, species, dynamics and conservation of energy. The iteration of the chemical turbulence of the gas phase was modeled from the Discrete Phase (MFD) model. In this method the reaction rates of both Arrhenius and Eddy-Dissipation are calculated and the net velocity is taken at least from these two rates, which is more realistic since it prevents reactants from burning as soon as they enter the computational domain. The reaction is modeled in two steps to model the homogeneous reaction of the gas phase. The turbulence model used is k-ε RANS, which demonstrated that this turbulence model provides a good agreement to predict the behavior of the reactive fluxes, due to the presence of solid particles of the flow.

Thus after evaporation, the mixture occurs by means of turbulence. however, the products generated by the combustion of the propellant are homogeneous, so the combustion gases obey the ideal gas law, the specific heat ratio (Cp/Cv) of the combustion gases is constant throughout the chamber, no heat is exchanged through the wall motor and the heat flow is adiabatic, and the temperature and pressure variation is only axial and the flow in the rocket outlet nozzle occurs in only one dimension in the x-direction.

4. NUMERICAL STUDY

In this paper a numerical study of the combustion of solid fuels was done, based on finite element methods in which some mathematical equations were considered that describe the movement of particles in the reactive flow are the transport equation. The adopted model has the conservative form of Eq. (D), considering that, within an infinitesimal control volume, the spatial variation is

$$\frac{\partial}{\partial t}\rho + \nabla . \rho \vec{V} = 0 \qquad \text{(D)}$$

Therefore, for the properties of the fluid system to be continuously transmitted through a volume, it can be described by momentum equation, which shortly after combustion is considered a

Newtonian fluid, then the exact Navier-Stokes EQ solution variables. Eq. (E) are decomposed into medium and floating components.

$$V_i = \bar{V}_i + V'_i \qquad \text{(E)}$$

The amount of motion of the compressible fluid equation adopted in this work is presented in equation Eq. (F).

$$\frac{\partial}{\partial t}(\rho V_i) + \frac{\partial}{\partial x_j}(\rho V_i V_j) = -\frac{\partial p}{\partial x_i} + \frac{\partial}{\partial x_j}\left[\mu\left(\frac{\partial V_i}{\partial x_j} + \frac{\partial V_j}{\partial x_i} - \frac{2}{3}\delta_{ij}\frac{\partial V_l}{\partial x_l}\right)\right] + \frac{\partial}{\partial x_j}\left(-\rho\overline{V_i' V_j'}\right) \qquad \text{(F)}$$

Thus, the left side of the equation represents the rate of change in the amount of movement that crosses the control surface per unit volume, the right side of Eq. (G) represents the external forces by volume units, which are those that act on the control volume as the fluctuation generated by the turbulence. CFD simulations of the combustion of potassium nitrate+pulverized sucrose were carried through the Eulerian-Lagrangian approach. Special attention was given to the modeling of turbulence in the continuous phase, using the RANS model.

To represent the temperature changes and eventual losses or heat gains that represent the energy variation, as well as the consumption and the production of species in the combustion process, the species and energy transport equations are presented below.

$$\frac{\partial}{\partial t}(\rho Y_k) + \nabla.(\rho V Y_k) = -\nabla.(\rho Y_k V_k) + \dot{\omega}_k \qquad \text{(G)}$$

One of the considerations that were made for the treatment of process thermochemistry is the reduction of one parameter: the mixing fraction, so this combustion simplification was adopted for the mixing problem. The mass fraction, f, is the mass fraction generated by the fuel in a given control volume, in the combustion reactions the masses of the chemical elements are conserved, then the equation of the mass fraction can be seen as the transport equation of the chemical fuel elements. A eq. (H) below represents the equation of the fraction of the mixture:

$$f = \frac{Z_k - Z_{k,ox}}{Z_{k,comb} - Z_{k,ox}} \quad \text{(H)}$$

Combustion reactions occur until the chemical equilibrium condition is reached. Considering that the temperature in the combustion process is high, the species of products are dissociated, producing several minority chemical species. The problem to be treated by the model is the calculation of the molar fractions of all the chemical species in the product of the combustion in a determined state of pressure and temperature, where the amount of matter of each chemical element is restricted. In this way, the number of atoms will remain the same. The free energy of Gibbs, "G", is commonly used. Only a few main points of the equation of the model were used, and its complete modeling can be found in references such as Turns (2000).

Gibbs free energy is defined as a function of the enthalpy, temperature, and entropy Eq. (I), the second law is then expressed in Eq. (J).

$$G = H - TS \quad \text{(I)}$$

$$(\mathrm{d}G)_{P,T,m} \leq 0 \quad \text{(J)}$$

Gibbs free energy is defined as a function of the enthalpy, temperature, and entropy Eq. (I) By demonstrating that Gibbs free energy decreases when some constant pressure or temperature change occurs. In this way, it is possible to calculate the chemical composition for various constant states of temperature and pressure. For example, if an ideal gas mixture for constant pressure, temperature and mass of species is considered; Eq. (K) looks like this:

$$\bar{g}_k(T) = \bar{g}^0(T) + TR_u ln\left(\frac{P_i}{P^0}\right) \quad \text{(K)}$$

Where $\overline{g}_k$ is the Gibbs function of the chemical species at the reference state pressure. Thus the reference pressure P0 was considered equal to 1 atm and Pi is the partial pressure, Ru is the ideal gas constant and T is the temperature. And the Gibbs function for an ideal gas mixture is expressed by Eq. (L).

$$G_{mist} = \sum N_k \bar{g}_{k,T} = \sum N_k [\bar{g}^0_{k,T} + R_u T ln\left(\frac{P_i}{P^0}\right)] \qquad \text{(L)}$$

The Kinetic energy accelerating a phase at the moment of combustion slows down, at the same time that the energy of a cloud influences an instability of the flow. When this is done, the expressions given, this phase corresponds to Eq. (M), As the concentration gradient changes, that is, the combustion being complete evaporates and reduces its radius; a thin layer of vapor fuel is being formed in proportion to the radiation around the camera and is heavily influenced by turbulence, so the more intense the turbulence, the higher the rate of mixing between the reactants.

$$\frac{\partial k}{\partial t} + U_j \frac{\partial k}{\partial x_j} = \tau_{ij} \frac{\partial U_i}{\partial x_j} - \beta^* k\omega + \frac{\partial}{\partial x_j}\left[(\nu + \sigma^* \nu_T)\frac{\partial k}{\partial x_j}\right] \qquad \text{(M)}$$

However in the combustion in turbulent flows, it was considered that the flow is governed by the momentum conservation equations, but due to the high computational time for the calculations. The species are described by the equations of the Reynolds averages. The program treated the turbulent flow in the premixed combustion from the diffusion gradient and the convection through the turbulent flow as a reinforcement of the diffusion effect. The Probability Density Function was used to derive the equations of Reynolds, species and energy averages for a single-point transport equation.

Where this function considered the fraction of time of each state of species, temperature and pressure in the flow. From the PDF, any thermochemical state at the single point. Thus the transport equation PDF composition is derived from the Navier-Stokes equations, represented in Eq (N), where P is Favre's joint PDF function, $.\overline{V}$ is the velocity vector, ω is the reaction rate of species k, Ψ is the spatial vector, V_i is the flotation velocity vector, $J_{i,j}$ is the vector of the molecular diffusion flux.

$$\frac{\partial}{\partial t}(\rho P) + \frac{\partial}{\partial x_i}\left(\rho \vec{V} P\right) + \frac{\partial}{\partial \Psi_k}(\rho \dot{\omega}_k P) = -\frac{\partial}{\partial x_i}\left[\rho \left\langle V_i^{''} \middle| \Psi \right\rangle P\right] + \frac{\partial}{\partial \Psi_k}\left[\rho \left\langle \frac{1}{\rho}\frac{\partial J_{i,k}}{\partial x_i} \middle| \Psi \right\rangle P\right. \qquad \text{(N)}$$

5. RESULT AND DISCUSSION

The results of the solid propellent combustion simulations were analyzed considering the same computational domain. The different velocity and temperature profiles were analyzed, corresponding to a range of falling diameter. In the region near the convergent-divergent nozzle we have a region, defined by the Radius decrease, the model captures results closer to those in the literature. Considering the same geometry and computational domain, the amount of air mass, corresponding to an ambient pressure of (25 °C) and an ambient pressure (1bar), was analyzed in the case of the reactive flow. The standard k-modelo model was used to predict the range, pressure, temperature and molar fraction of each element in which the reactive flow of the combustion reaction was studied, in which the largest product is Water (H_2O) and Dioxiod of Carbon (CO_2).

The case of non-reactive flow was simulated and analyzed by varying the amount of propellant mass as a function of the reaction time. were selected for this comparison because they are the minimum and maximum reaction velocity values studied in this work. The standard κ-modelo model was used in this study to predict the runoff field and its results were compared. The results of the combustion in which it was 8.5 seconds of combustion were analyzed, were analyzed in 3 times, where it passed to 0, 4, 8 seconds, where it was considered 8.5 according to the final combustion time, so that there was no further reaction .

In figure 5, 6, 7, the pressure distribution was analyzed along the geometry, at the time of 0, 4 and 8 seconds respectively.

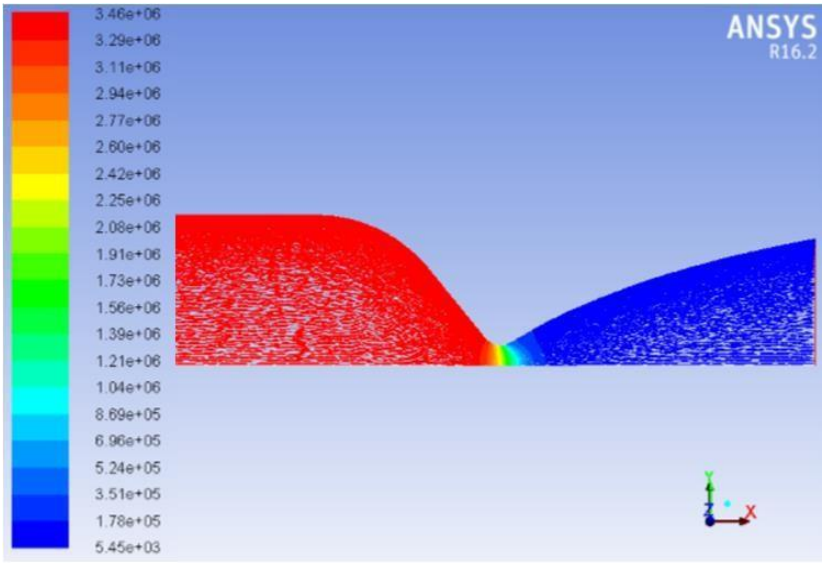

Figure 5 - Pressure distribution along full geometry.

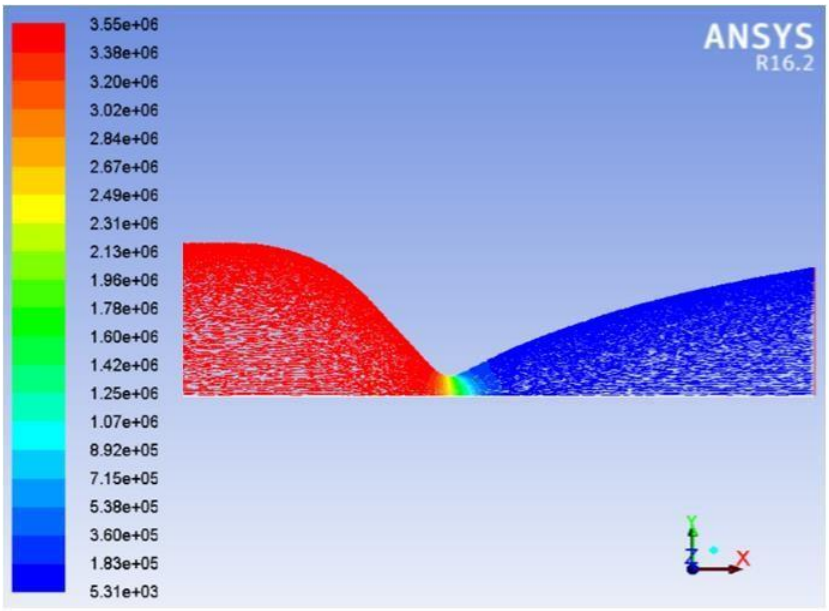

Figure 6 - Pressure distribution along full geometry.

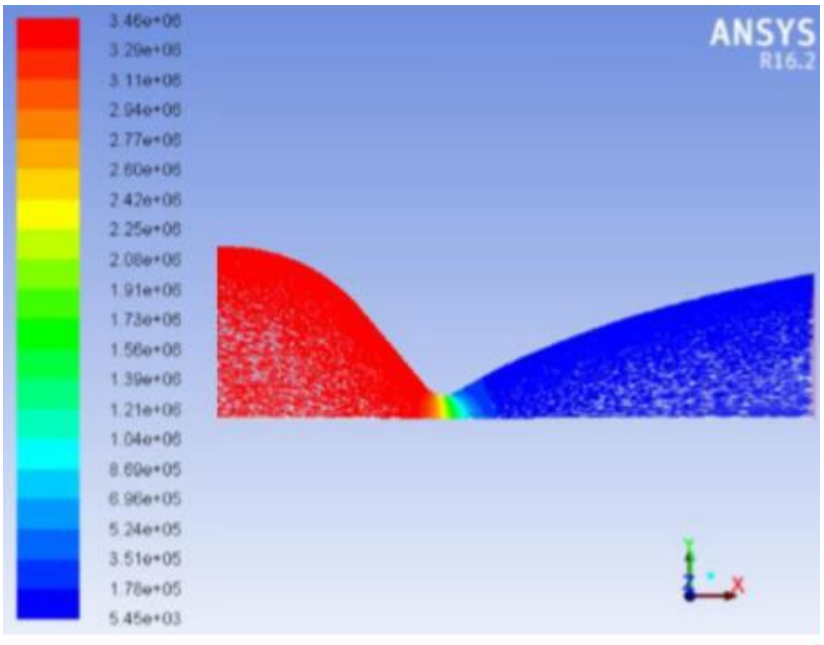

Figure 7 - Pressure distribution along full geometry

It can be seen in Figure Where standard κ-utilizado was used that in the region near the exit nozzle there are areas of high pressure in a small area, generating a positive pressure which characterizes a region of laminar flow, it is possible to verify that the pressure fields had at all time analyzed results with greater precision. It is observed a better detailed pressure variations, this is because this model has the characteristic to predict more accurately the dissipation rate in axissimetric flows In Figure 8.9.10, it is possible to verify the temperature in the time of 0, 4 and 8 seconds, respectively.

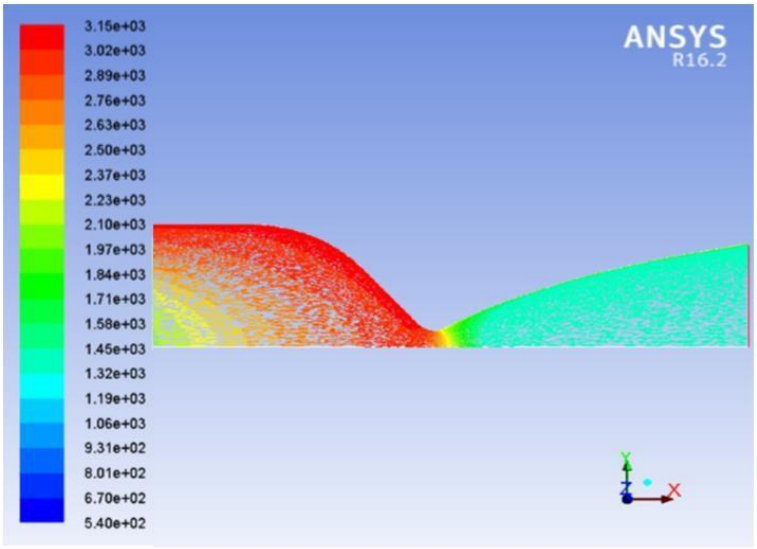

Figure 8 - Temperature distribution along the complete

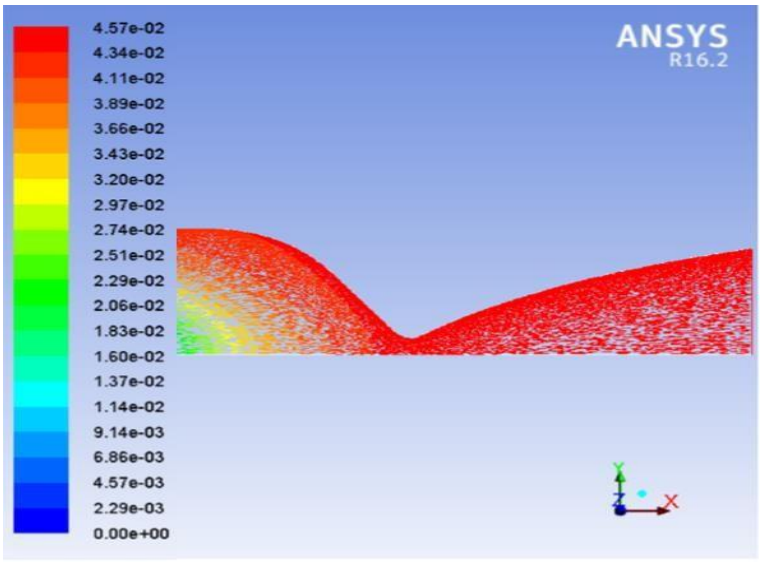

Figure 9 - Temperature distribution along the complete

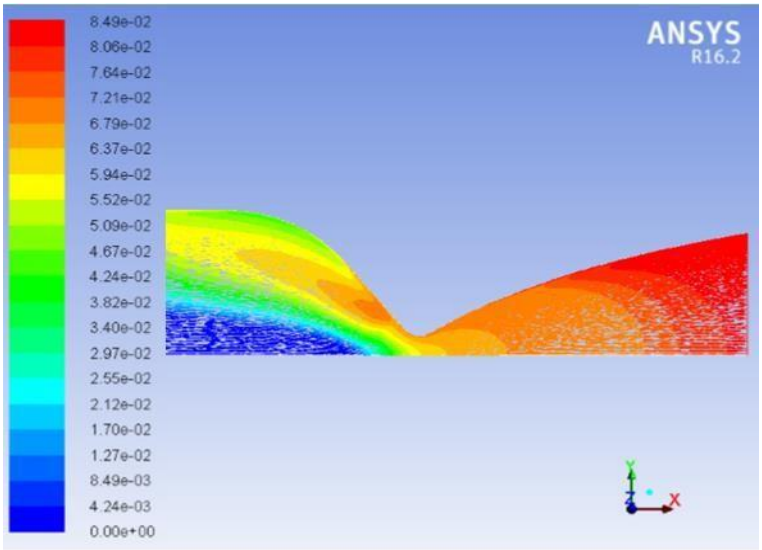

Figure 10 - Temperature distribution along the complete

The way the fuel is consumed in the engine has a significant influence on the shape of the heating in the near points of the engine wall and in the laval mouth, it is possible to observe that the increase in temperature over time is greater, this is proved, since it is consequently in the process of combustion and flame formation, since in this case sucrose provides greater energy efficiency in the combustion. The propellant studied here is on the surface with an amount of movement equal to zero, causing the fuel material to pass through the three solid-liquid-gaseous states, which in the last stage are diluted in the flow and by the air that accelerates and drags them.

The distribution of the temperature field shows the formation of the flame very close to the outlet nozzle, which can be observed by the temperature gradient difference. In the vicinity of the outlet nozzle, the highest temperatures were recorded, because it is in this region immediately next that the amount of fuel is higher and with higher speed flow, the evaporation of the propellant occurs rapidly, that is, the amount of fuel vapor increases rapidly in this region by combining this feat with the submerged solids particles and also the increase in temperature of the air caused by the convection effect resulting from the relative velocity between the gaseous and discrete phase causes the mixing fraction to rapidly increase near the outlet nozzle , consequently a high temperature as seen in Figure 11.

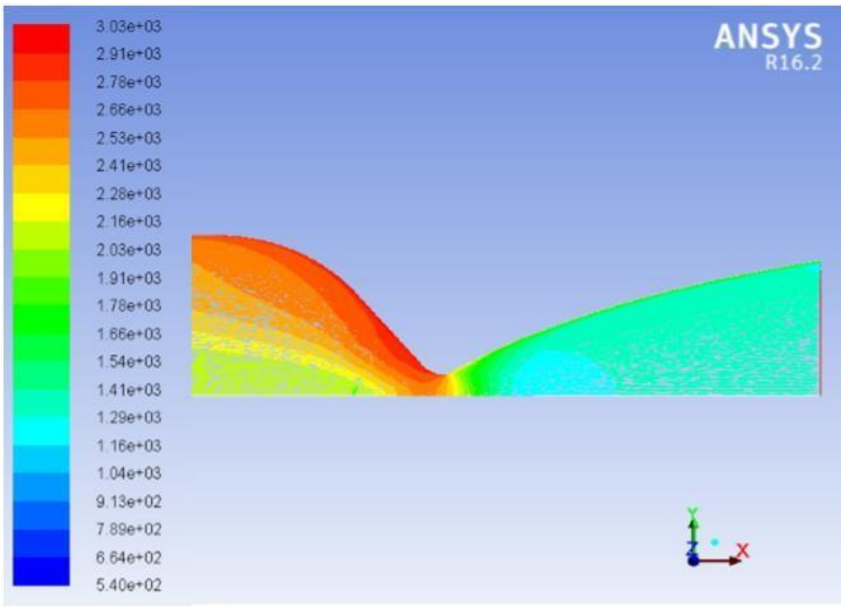

Figure 11 - Distribution of carbon dioxide along the complete geometry

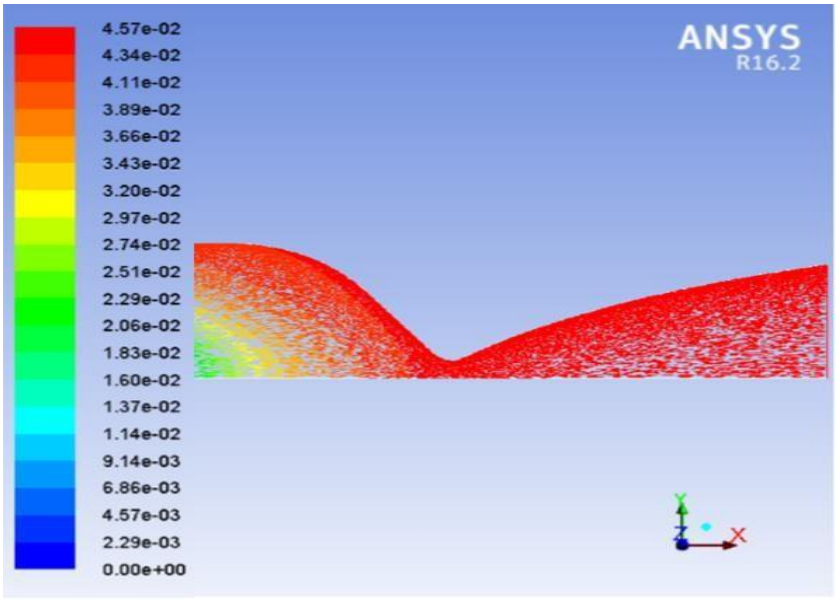

Figure 12 - Distribution of carbon dioxide along the complete geometry.

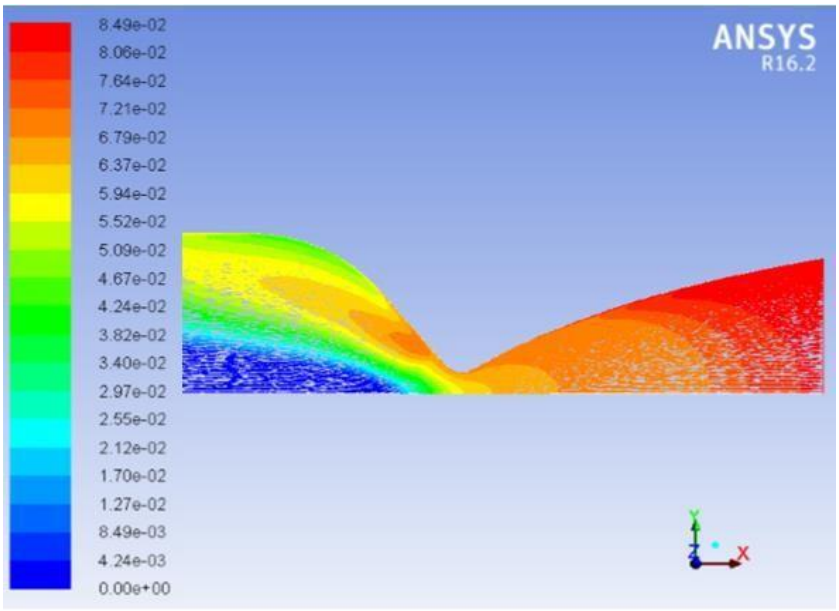

Figure 13 - Distribution of carbon dioxide along the complete geometry.

Fig. 11,12 and 13 show the distribution of CO_2 mass fraction during the time of 0, 4 and 8 seconds, respectively. This chemical species was defined for analysis as being highly polluting. The chemical species CO_2 of the hydrocarbon combustion reaction is the final product, this is one of the gases which contributes to increase the pressure in the engine chamber and as it is formed it is expelled thus further aiding in the rocket's thrust.

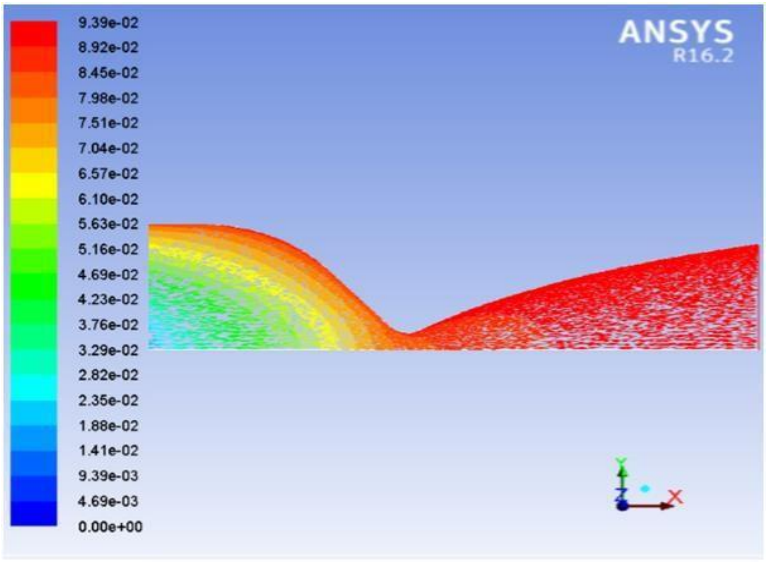

Figure 14 - Distribution of water along full geometry.

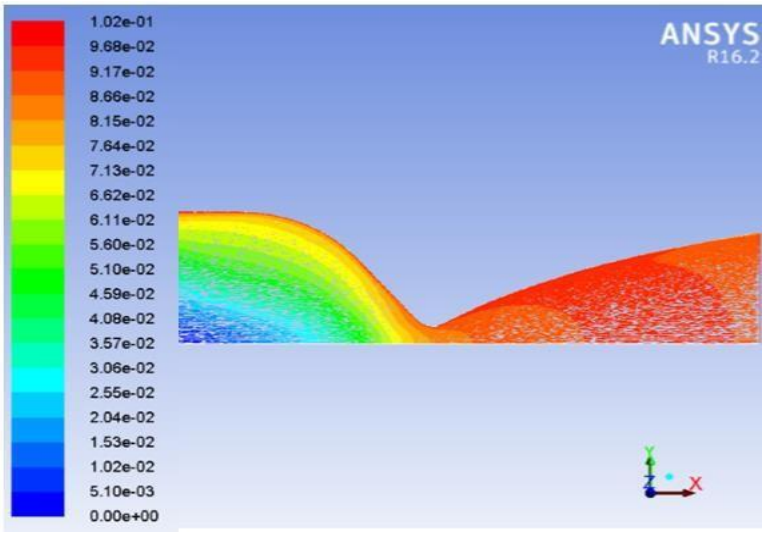

Figure 15 - Distribution of water along full geometry.

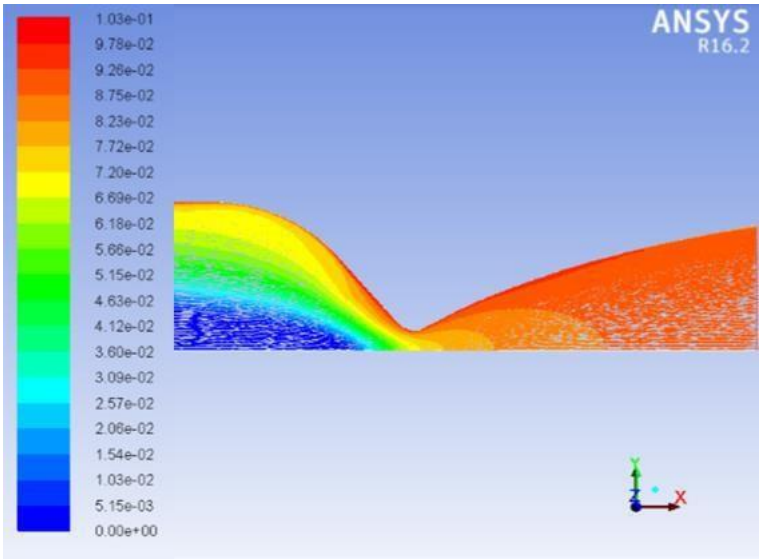

Figure 16 - Distribution of water along full geometry.

Fig. 14,15 and 16 presents the results for distribution H2O concentration fraction. shows the distribution of the water vapor concentration range, which is also a final product of complete combustion. The regions with the highest concentration of H_2O are close to the vicinity of the nozzle and flame region, where the combustion reaction occurs. It is observed that the behavior of the H_2O mass fraction concentration is similar to field of fractional mass de CO_2.

The simulated results showed that the values of the exhaust velocity and the combustion temperature obtained during the simulation are in agreement with the values found in the literature. The products of the propellant burning reaction are mainly carbon dioxide, and water. As can be seen, in the analysis of the ansys package, as soon as the flow begins, the reaction and the high temperature region, which extends from the fuel and oxidant inputs to the axis of symmetry, begin immediately.

It is interesting to note the change in behavior of the properties over time during the combustion process inside the combustion chamber. When comparing the 3 time slots, the very high temperature gradients in the system due to the permanent state. Around the entrance, temperatures rise from 298K to 2000K at close distances, it is also possible to observe that the peak pressure decreases by about 1 bar every 4 seconds.

The maximum temperature in the convergent part of the nozzle also has its maximum value initially of 588.15 K, and every 4 seconds it decreases around 100 K. The velocity of the sound behaves in a similar way to the temperature because they are directly related . Finally, the velocity and Mach number have maximum values initially and gradually decrease with the passage of time.

The simulation was successful, demonstrating that the simulation used to predict the performance of a solid rocket engine is a safe and viable alternative for the development of rocket engines. The variation of the values of the chemical elements is also very coherent, along with the deliberate properties in the initial condition. The combustion products initially have the largest distribution at the exit of the nozzle and in the convergent part, over time this concentration decreases, which is explained by the reduction of the combustion process, that is, $C_{12}H_{22}O_{11} + KNO_3$, which is burned in the time of 8.5 seconds and forming the product $CO_2 + H_2O$.

6. CONCLUSION

In this work, a study was conducted in a turbulent flow of a combustion of solid propellant potassium nitrate / sugar to rocket motor as solid fuel. The behavior of the velocity field was observed in the combustion reaction. The simulated results showed that the values of the exhaust velocity and the combustion temperature obtained during the simulation are in agreement with the values found in the literature. The products of the propellant burning reaction are mainly carbon dioxide, and water. as can be obtained through the analysis package, as the combustion begins, the high temperature region, extends from the motor walls out of the laval nozzle.

In addition, it was realized that improvements in the flame velocity behavior were observed so that it could be applied in a method to obtain a complete burn and not generate solid particles in the outlet nozzle, this is possible by applying a balance in the amount of nitrate and sucrose, another possibility is the use of other fuels in which there will be no partial burning.

The possible reduction of the equivalence ratio at the exit of the nozzle nozzle can modify the behavior of the flame reducing it as well as the CO and CO2 levels. The chemical kinetics mechanisms used in the simulations presented significant influence on the results of the temperature fields and the flame formation.

The failure of the values of the chemical elements is also very consistent along with the antecedent properties. The combustion products initially have the largest distribution at the exit of the nozzle and in the convergent part, over time this concentration decreases, which in practice is explained by the reduction of the feed of the combustion process, ie, it is being burned along of time.

In this case it was not considered the temporal variation of its flow and the propellant, which should occur in practice due to the variation of the pressure of the camera and the burning of the fuel.

ACKNOWLEDGMENT

The authors would like to thank the Federal University of Pará (UFPA), Tutorial Education in Mechanical Engineering Program (PETMEC) and the National Fund for the Development of Education (FNDE) for financial assistance.

REFERÊNCIAS

BALDISSERA, R.; GABRIEL, L.; POLETTO, M. Propelentes sólidos para foguetes - Avaliação da geração de gases tóxicos com base nas reações de combustão. **5º Congresso Internacional de Tecnologias para o Meio Ambiente**, Bento Gonçalves, 2016.

BARRÈRE, M.; JAUMOTTE, A.; VANDENKERCKHOVE, J.; Rocket Propulsion, **Elsevier Publishing Company**, 2nd Edition, 1960.

CARTER, M.G. An investigation into the combustion and performance of small solid-propellant rocket motors. **Final Thesis Report.** University of New South Wales. 2008; 1-34.

CORNELISSE, J. W.; SCHOYER, H. F. R.; WAKKER, K. F.: **Rocket Propulsion and Spaceflight Dynamics**, Pitman London, 1979.

FOLTRAN ,A. C. MORO, D .F, SILVA N.D.P, FERREIRA, A.E.G, ARAKI, L. K , MARCHI, C. H, **Burning Rate Measurement of KNSu Propellant Obtained by Mechanical Press**, 2015

GUTHEIL, E. 2011. Issues in Computational Studies of Turbulent Spray Combustion. Experiments and Numerical

PETERSON, P. H. C.; **Mechanics And Thermodinamics of Propulsion**, 2nd edition,1992.

LENGELLÉ, G.; DUTERQUE, J; TRUBERT, J.F. "Physico-Chemical Mechanisms of Solid Propellant Combustion". Contribution to "Solid Propellant Chemistry, Combustion and Motor Interior Ballistics", **Volume 185, Progress in Astronautics and Aeronautics,** AIAA, 2000.

NAKKA, R. KN. **Sucrose propellant chemistry and performance characteristics.** Richard Nakka's Experimental Rocketry Web Site. 1999.

SHMAKOV, A.G., KOROBEINICHEV, O.P. & BOL'SHOVA, T.A. Combustion, Explosion, and Shock Waves (2002) 38: 284. https://doi.org/10.1023/A:1015697618376

SUTTON, G. P.; **Rocket Propulsion Elements: An introduction to the enginneering of rockets**, 2001.

VYVERMANN, T. **The potassium nitrate – sugar propellant**. Relatório, 1978.

WEISS, W.; SESSLER, J. G.; Aerospace Structural Metals **Handbook, Vol. I**, Syracuse Univerity, Research Center, 1963.

YANG V., BRILL T.B. and REN W.Z., **Solid Propellant Chemistry, Combustion and Motor Interior Ballistic**, Volume 185 of Progress in Astronautics and Aeronautics, 2000.